ORGANOMETALLICS

Article

Cite This: Organometallics 2019, 38, 3187−3196

pubs.acs.org/Organometallics

Mechanistic Complexity of Asymmetric Transfer Hydrogenation with Simple Mn−Diamine Catalysts

Robbert van Putten,[†] Georgy A. Filonenko,[†] Angela Gonzalez de Castro,[‡] Chong Liu,[†,⊥] Manuela Weber,[§] Christian Müller,[§] Laurent Lefort,[‡] and Evgeny Pidko*[,†,∥]

[†]Inorganic Systems Engineering Group, Department of Chemical Engineering, Faculty of Applied Sciences, Delft University of Technology, Van der Maasweg 9, 2629 HZ, Delft, The Netherlands

[‡]InnoSyn B.V, Urmonderbaan 22, 6167 RD, Geleen, The Netherlands

[§]Freie Universität Berlin, Institute of Chemistry and Biochemistry, Fabeckstrasse 34/36, D-14195 Berlin, Germany

[∥]TheoMAT Group, ChemBio Cluster, ITMO University, Lomonosova str. 9, Saint Petersburg, 191002, Russian Federation

Supporting Information

ABSTRACT: The catalytic asymmetric transfer hydrogenation (ATH) of ketones is a powerful methodology for the practical and efficient installation of chiral centers. Herein, we describe the synthesis, characterization, and catalytic application of a series of manganese complexes bearing simple chiral diamine ligands. We performed an extensive experimental and computational mechanistic study and present the first detailed experimental kinetic study of Mn-catalyzed ATH. We demonstrate that conventional mechanistic approaches toward catalyst optimization fail and how apparently different precatalysts lead to identical intermediates and thus catalytic performance. Ultimately, the Mn−N,N complexes under study enable quantitative ATH of acetophenones to the corresponding chiral alcohols with 75−87% ee.

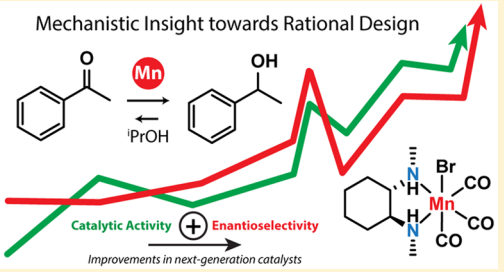

INTRODUCTION

Homogeneous hydrogenation catalysis with earth-abundant 3d transition metals (TMs) such as Fe, Co, and Mn has received remarkable attention from the catalytic community in recent years as a benign and sustainable alternative to processes involving noble metals.[1,2] This increased focus has led to the rapid development of highly potent first-row transition metal catalysts for a vast number of transformations involving hydrogen-transfer steps, such as hydrogenations, dehydrogenations, and coupling reactions.[3−7] While Ru and Ir remain the conventional metals for these reactions,[8] several examples have emerged of early TMs matching or even surpassing the catalytic activity of noble metals, highlighting the vast chemical potential of this class of homogeneous catalysts.[9−12]

In addition, first-row TM catalysts exhibit striking reactivity patterns unprecedented in hydrogenation catalysis.[3,5,13,14] A chemically distinct feature of some manganese hydrogenation catalysts is that they do not rely on commonly employed strong donor ligands such as phosphines.[15,16] Indeed, for Mn, the introduction of simple bi- or tridentate nitrogen-donor ligands was sufficient to promote hydrogenation of carbon dioxide to formate and formamide[17] and transfer hydrogenation of C═X bonds (X = O, N), e.g., ketones, imines, and aldimines.[18−25]

In order to understand the origin of catalytic activity and causes for the current limitations of Mn systems, we carried out a detailed mechanistic and kinetic study of Mn catalysts in the asymmetric transfer hydrogenation of ketones. The groups of Kirchner,[26] Clarke,[27] Beller,[28,29] and Morris[30] reported the use of Mn catalysts bearing multidentate phosphine ligands for the asymmetric hydrogenation of ketones. However, we decided to focus on simpler diamine-based Mn catalysts, as were reported by Sortais and co-workers.[31] From a practical and cost point of view, we deemed these catalysts attractive candidates for industrial applications,[32,33] as the active system could be generated in situ and was shown to achieve the ATH of a large scope of aryl ketones. After an extensive screening of (chiral) diamines, the combination of 1 mol % $Mn(CO)_5Br$ and ligand **(1*R*,2*R*)-*N*,*N*′-Me$_2$-DPEN** was identified as the most potent, ultimately enabling good to quantitative yields of corresponding alcohols with 30−90% enantiomeric excess (ee) (Scheme 1).

Scheme 1. Chiral Mn−N,N Catalysts for Asymmetric Transfer Hydrogenation of Ketones

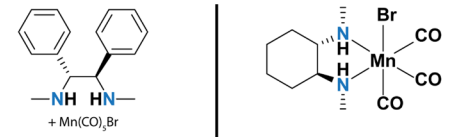

(1*R*,2*R*)-*N*,*N*′-Me$_2$-DPEN — Sortais[31]

(1*S*,2*S*)-*N*,*N*′-Me$_2$-DACH — This work

Received: July 4, 2019
Published: August 15, 2019

DOI: 10.1021/acs.organomet.9b00457
Organometallics 2019, 38, 3187−3196

Scheme 2. Screening of In-Situ Manganese−N,N and Manganese−P,N Catalysts for Asymmetric Transfer Hydrogenation of Acetophenone[a]

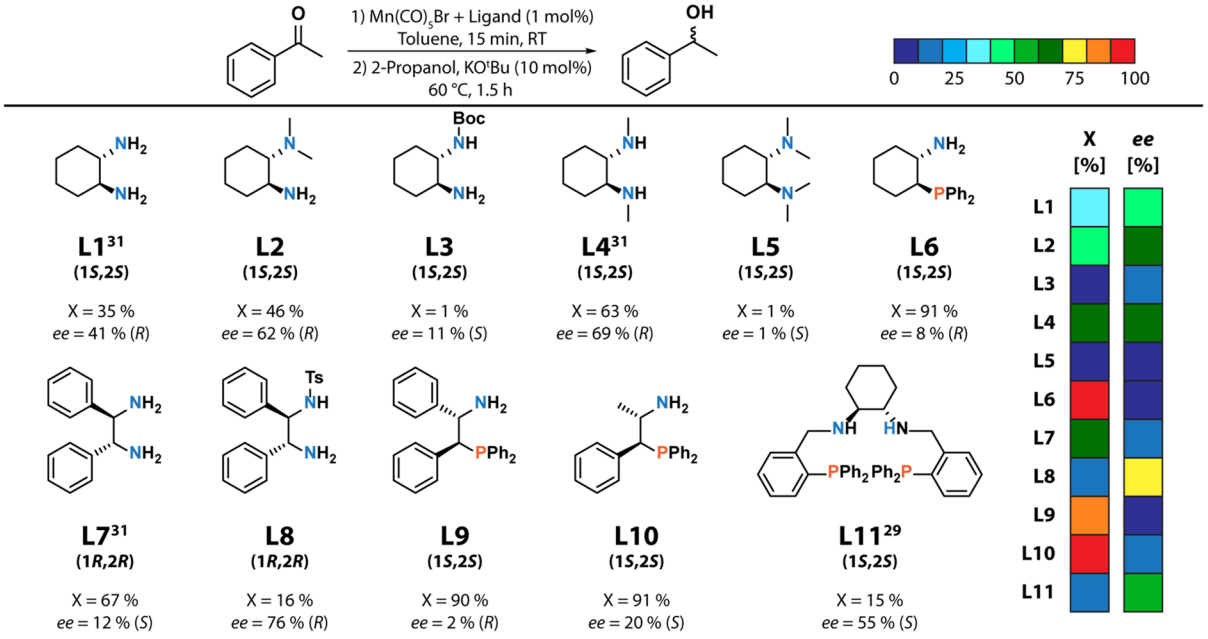

[a]Conditions: 0.5 mmol of acetophenone, 10.0 mol % KO^{t}Bu, 1.0 mol % Mn(CO)$_5$Br, 1.0 mol % ligand, 2.5 mL of ^{i}PrOH + 0.5 mL of toluene, 60 °C, 1.5 h. Yields determined by GC-FID using *n*-dodecane as an internal standard. A number of ligands have been evaluated before under slightly different conditions (see refs 29 and 31).

Scheme 3. Synthesis of Well-Defined Mn Precatalysts 1-*Cis* and 1-*Trans*[a]

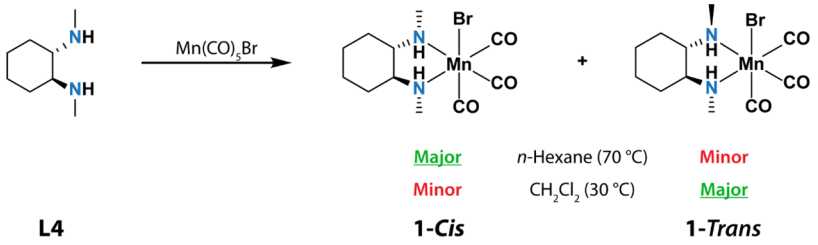

[a]The mixture of *cis* and *trans* is denoted as **1**.

Thus far, the open literature does not provide substantial mechanistic analysis of Mn-catalyzed ATH due to the lack of isolated or well-defined bidentate Mn complexes for the asymmetric transfer hydrogenation of ketones. Herein, we describe the identification, isolation, and characterization of a series of simple chiral Mn−diamine catalysts. The combination of stoichiometric reactivity studies, DFT calculations, and analysis of reaction kinetics allowed the complex reactivity patterns of apparently simple Mn−N,N catalysts to be identified in the asymmetric transfer hydrogenation of ketones.

In-Situ Screening and Precatalyst Isolation. We began our studies by evaluating a series of readily available chiral diamines and aminophosphines as ligands for the Mn-catalyzed ATH of acetophenone (Scheme 2). The Mn complexes were prepared by stirring Mn(CO)$_5$Br with 1 equiv of the chiral ligand in toluene at room temperature for 15 min. The toluene solution with the Mn/L-combination was transferred into ^{i}PrOH containing the substrate and KO^{t}Bu as a base. In these initial experiments, a catalyst loading of 1 mol % with respect to acetophenone was used, while base was present at 10 mol %.

The highest catalytic activities were observed for bidentate aminophosphine ligands **L6**, **L9**, and **L10**, unfortunately with low ee's not exceeding 20%. In contrast, a high enantiomeric excess of 76% was achieved with tosyl protected DPEN ligand **L8** but at a much lower conversion compared to the unprotected DPEN ligand **L7**. Interestingly, dialkylated diaminocyclohexanes (**L2** and **L4**) led to modest catalytic activity combined with good enantioselectivity, whereas nonalkylated analogue **L1** was less active and selective, and tetra-alkylated ligand **L5** showed no activity at all.

Having identified *N*,*N*′-dimethyl 1,2-diaminocyclohexane **L4** as the best ligand in our initial evaluation in terms of the trade-off between activity and enantioselectivity, we sought to isolate the precatalyst formed upon complexation of **L4** to Mn(CO)$_5$Br (Scheme 3). The corresponding complex **1** was readily formed upon refluxing in *n*-hexane for several hours and was obtained in 34% yield after recrystallization from DCM/*n*-hexane/diethyl ether at −20 °C. The compound was fully characterized using ^{1}H/^{13}C NMR, FT-IR, elemental analysis, and single-crystal X-ray analysis (see the Supporting Information).

Upon complexation, the methyl groups in **L4** lose equivalency and appear in ^{1}H NMR of **1-*Cis*** as two sharp doublets at δ = 2.9 ppm and δ = 2.7 ppm in CD_2Cl_2. We

DOI: 10.1021/acs.organomet.9b00457
Organometallics 2019, 38, 3187−3196

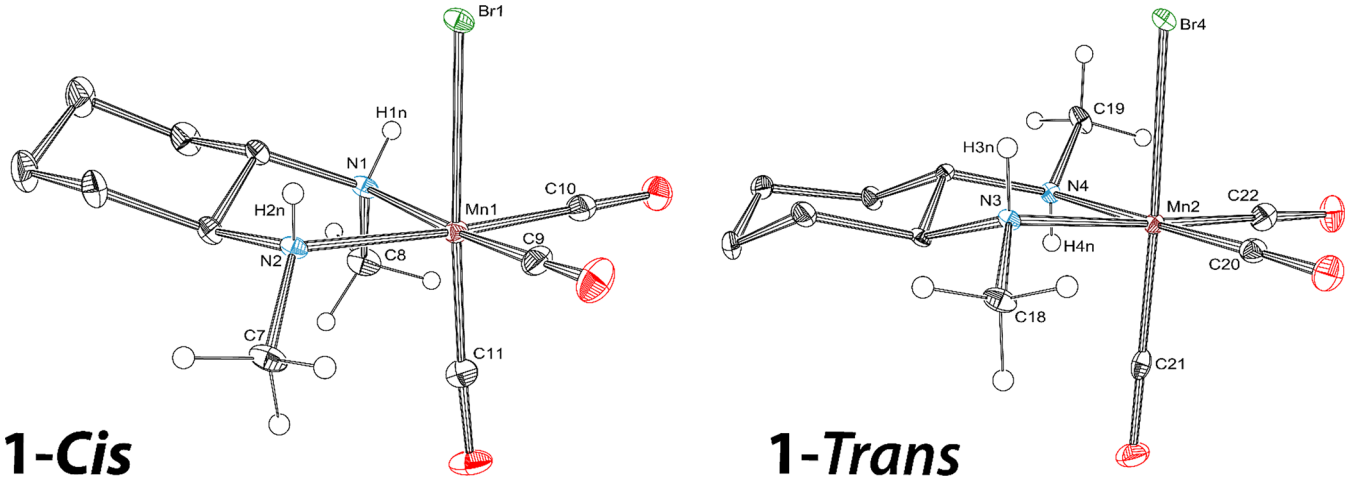

Figure 1. ORTEP diagrams of **1-*Cis*** (left) and **1-*Trans*** (right). Thermal ellipsoids are drawn at 30% probability. Co-crystallized solvent and hydrogen atoms (except bound to nitrogen and N−Me) have been omitted for clarity.

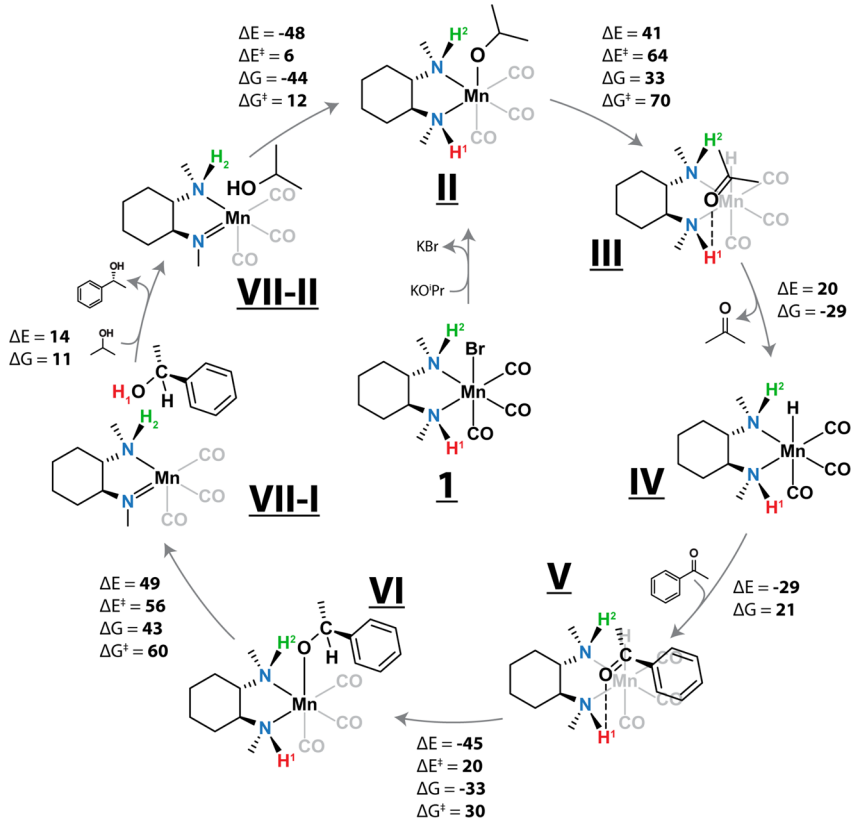

Figure 2. Proposed catalytic cycle for asymmetric transfer hydrogenation with **1-*Cis***. ΔG and $G^{\ddagger}$ represent reaction and activation Gibbs free energy changes in kJ mol^{-1} at 333 K, respectively. Cycle for formation of (*R*)-product shown.

hypothesize that the observed dissimilarity of the methyl groups originates from the locked chair conformation of the cyclohexane ring due to chelation to Mn. The different steric environments of the axially and equatorially bound nitrogen atoms (i.e., varied proximity to ring-bound C−*H*) lead to the observation of the two distinct signals. The N*H* resonances of **1-*Cis*** are present as two broad singlets at δ = 3.3 ppm and δ = 2.6 ppm, further indicating the chemical inequivalence of the amino groups (see the Supporting Information for full characterization).

Under the selected reaction conditions, we could observe the formation of a secondary product that has a distinct ^{1}H NMR spectrum from **1-*Cis***. This complex features a ^{1}H NMR spectrum in which resonances from the N*H* and N−Me groups overlap and produce a band of signals between δ = 3.0−2.8 ppm. This compound could be separated from **1-*Cis*** by slow vapor diffusion crystallization from the original mother liquor by further addition of *n*-hexane (see the Supporting Information, **1-*Trans***, procedure A).

Single-crystal X-ray diffraction data of both products revealed their identities as *cis* and *trans* isomers. The solid-state structure of **1-*Cis*** features the methyl groups bound in *cis* fashion, both oriented in opposite direction to the bromide ligand bound in the axial position of octahedral complex **1-*Cis***

DOI: 10.1021/acs.organomet.9b00457
Organometallics 2019, 38, 3187−3196

Scheme 4. DFT Calculations into the Origin of Enanantioselectivity of Catalysis with Mn−Hydrides V−H[1] and V−H[2] [a]

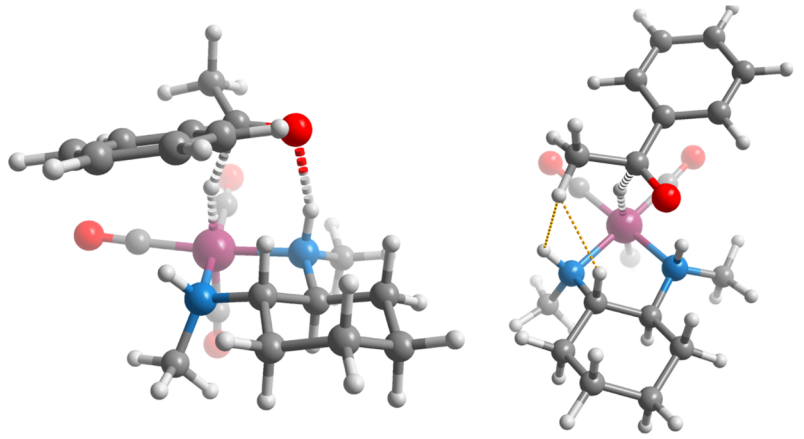

V-H[1] / *Si* / (*R*)
Favorable

V-H[1] / *Re* / (*S*)
Unfavorable

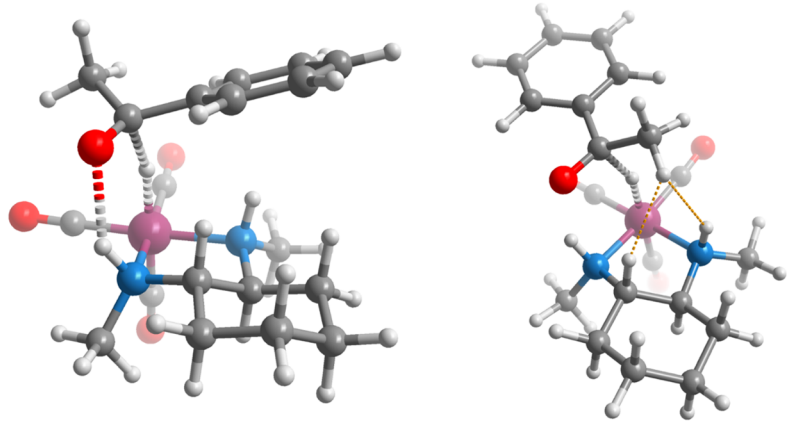

V-H[2] / *Re* / (*S*)
Favorable

V-H[2] / *Si* / (*R*)
Unfavorable

Product	1-*Cis*				1-*Trans*	
	Reaction Site (H[1])		Reaction Site (H[2])		Reaction Site (H[1])	
	ΔE‡	ΔG‡	ΔE‡	ΔG‡	ΔE‡	ΔG‡
(*R*)-1-Phenylethanol	20	**30**	31	44	20	**33**
(*S*)-1-Phenylethanol	26	40	22	**39**	25	**40**

[a]Dotted yellow lines highlight steric interactions of unfavorable high-energy TS.

(Figure 1). The second product was identified as **1-*Trans***, a minor isomer (<20%) of **1** in which the N*H* protons are oriented *trans* (Figure 1). The ratio of **1-*Cis*/1-*Trans*** was found to be strongly dependent on the complexation conditions; a nearly inverse ratio of **1-*Cis*/1-*Trans*** was obtained when the reaction was performed in dichloromethane at 25 °C (Scheme 3).

Isomers **1-*Cis*** and **1-*Trans*** did not interconvert upon prolonged heating at 70 °C in THF-d_8 or C_6D_6, indicating that their formation and relative abundance is a kinetic ratio governed by synthetic conditions rather than chemical exchange phenomena. Additionally, no ligand substitution occurred when **1-*Cis*** or **1-*Trans*** was refluxed in benzene in the presence of 2 equiv of triphenylphosphine, further confirming their thermal and chemical stability. The presence of a 2-fold **L4** excess during complexation did not result in the formation of cationic $[Mn(L)_2(CO)_2]^+$ species, which are frequently observed when stronger phosphine-donor ligands are utilized.[27,28,34]

With the isolated complexes **1-*Cis*** and **1-*Trans*** in hand, we tested whether they would have different catalytic performances. Both complexes, however, produced a virtually identical yield of (*R*)-1-phenylethanol of ∼40% in 1 h at 60 °C with 74% ee, which is a slight improvement in performance over the situation when the catalyst was generated in situ (Table S2). Preactivation of precatalysts **1-*Cis*** and **1-*Trans*** with $NaHBEt_3$[30,35] allowed the catalytic reaction to be operated base free. Catalytic performance was not improved and was identical for both complexes, again indicating that the catalytically active species formed from precatalysts **1-*Cis*** and **1-*Trans*** are identical.

Mechanistic Investigations and Origin of Stereoselectivity. We next employed density functional theory (DFT) to rationalize the observed trends in catalysis with complexes **1-*Cis*** and **1-*Trans***. The reaction mechanism was

DOI: 10.1021/acs.organomet.9b00457
Organometallics 2019, 38, 3187−3196

Scheme 5. Stoichiometric Reactivity Studies with Complexes 1-*Cis* and 1-*Trans*

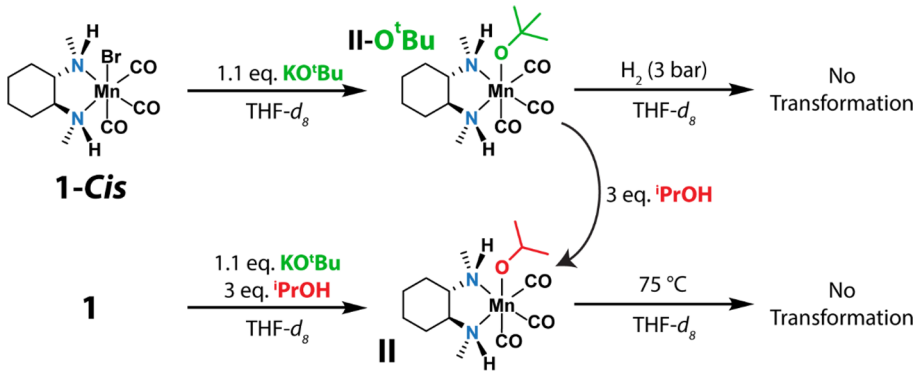

Scheme 6. Isolated Chiral Manganese−Diamine Complexes

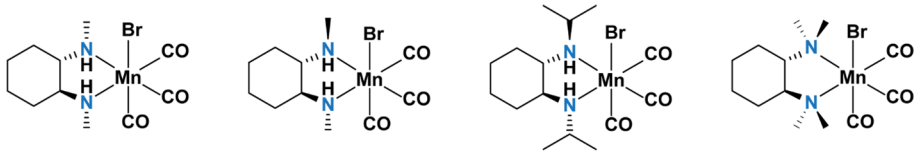

investigated at the PBE0-D3(BJ)-SMD(^{i}PrOH)/Def2QZVPP level of theory using the Gaussian 09 D.01 program.[36] The proposed catalytic mechanism as well as reaction and standard activation Gibbs free energies for elementary steps are summarized in Figure 2.

The catalytic cycle starts by activation of precatalyst **1-*Cis*** with KO^{t}Bu and ^{i}PrOH (or KO^{i}Pr, created in situ) to form Mn−isopropoxide complex **II**, which is a resting state in the catalytic cycle. β-Hydride elimination of the anionic isopropoxide ligand with concomitant formation of Mn−hydride complex **III** proceeds with the highest activation Gibbs free energy in the catalytic cycle of 70 kJ mol^{-1}. Acetone is removed from **III** to produce catalytically active Mn−hydride **IV**. The ketone substrate subsequently coordinates to **IV** via N*H*-assisted hydrogen bonding, forming Mn-adduct **V**, and reacts endergonically ($\Delta G^{\ddagger}_{(R)}$ = 30 kJ mol^{-1}, $\Delta G^{\ddagger}_{(S)}$ = 39 kJ mol^{-1}) through enantiodetermining hydride transfer, leading to the formation of Mn−alkoxide resting state **VI**. Liberation of the 1-phenylethanol product is an activated process with a high barrier of 60 kJ mol^{-1} and results in the formation of reactive Mn−amido intermediate **VII−I**. Deprotonated complex **VII−II** readily reacts with free ^{i}PrOH in an exergonic reaction with a low barrier of only 12 kJ mol^{-1} to regenerate MnO^{i}Pr species **II** and complete the catalytic cycle.

Cis-complex **1-*Cis*** possesses two accessible and reactive N−*H* moieties (H^1 and H^2 in Figure 2), whereas *trans*-ligated systems only bear one (H^1). The steric environment of both N−*H*'s, however, is different because of the close proximity of up-and-down oriented carbon/hydrogen atoms in the cyclohexyl ring (Scheme 4). This difference potentially impacts stereoselectivity, as it may lead to preferential precoordination of the *Re* or *Si* face of acetophenone to **1-*Cis*** and **1-*Trans***. We therefore studied the enantiodeterminative step in more detail using DFT and calculated the energies for coordination of the *Re* and *Si* faces of acetophenone to all reactive protons, i.e., four combinations for **1-*Cis*** and two for **1-*Trans*** (Scheme 4). These studies revealed preferential formation of (*R*)-1-phenylethanol for both conformers which originates from coordination of the *Si* face to proton H^1. Enantioselective induction is predominantly achieved through steric repulsion between the substrate CH_3 and nearby ligand-bound C*H* and N*H* (transition states for **1-*Cis*** shown in Scheme 4).

The differences in activation barriers for the transfer of proton H^1 are 9 and 7 kJ mol^{-1} between H^1 and H^2 for *cis* and *trans* **V**−hydrides, respectively (details in Scheme 4 and the Supporting Information). Thus, reaction at H^2 is a more activated process and results in (*S*)-alcohols. Calculated results correctly predict the preferential formation of the major (*R*) enantiomer found experimentally and, contrary to our original hypothesis, predict virtually identical enantioselective performance of **1-*Cis*** and **1-*Trans***.

A stoichiometric reactivity study was performed using ^{1}H NMR spectroscopy to experimentally substantiate results obtained with DFT. Reaction of **1-*Cis*** and KO^{t}Bu in THF-d_8 (i.e., in the absence of ^{i}PrOH) led to the formation of a new octahedral Mn−alkoxide complex **II−O^{t}Bu** (Scheme 5, top), evidenced by the significant change of the ^{1}H NMR spectrum (Figure S18). Addition of ^{i}PrOH to a solution of **II−O^{t}Bu** in THF-d_8 resulted in a rapid color change of the reaction mixture from red to yellow, associated with the formation of the Mn−isopropoxide complex **II**. The identity of neutral complex **II** is suggested on the basis of ^{1}H NMR, indicated by the appearance of a new resonance at δ = 4.07 ppm that is assigned to the Mn-bound isopropoxide moiety. Interestingly, the ^{i}PrO anion in **II** is dynamic and rapidly exchanges with free ^{i}PrOH in solution, as evidenced by 2D-NOE measurements (Figure S34). The same *cis*-Mn−alkoxides **II−O^{t}Bu** and **II** were formed upon treatment of **1-*Cis*** or **1-*Trans*** with KO^{t}Bu in the absence of ^{i}PrOH (**II−O^{t}Bu**) or with ^{i}PrOH (**II**). This observation implies that the treatment of **1-*Trans*** with KO^{t}Bu converts it into a complex where both protons and methyls are in a *cis*-configuration. Consequently, both isomers **1-*Cis*** and **1-*Trans*** show an identical catalytic reactivity and selectivity in the ATH reaction.

Interestingly, even in the presence of minor quantities ^{i}PrOH (ca. 2−3 equiv), Mn−isopropoxide complex **II** appears

DOI: 10.1021/acs.organomet.9b00457
Organometallics 2019, 38, 3187−3196

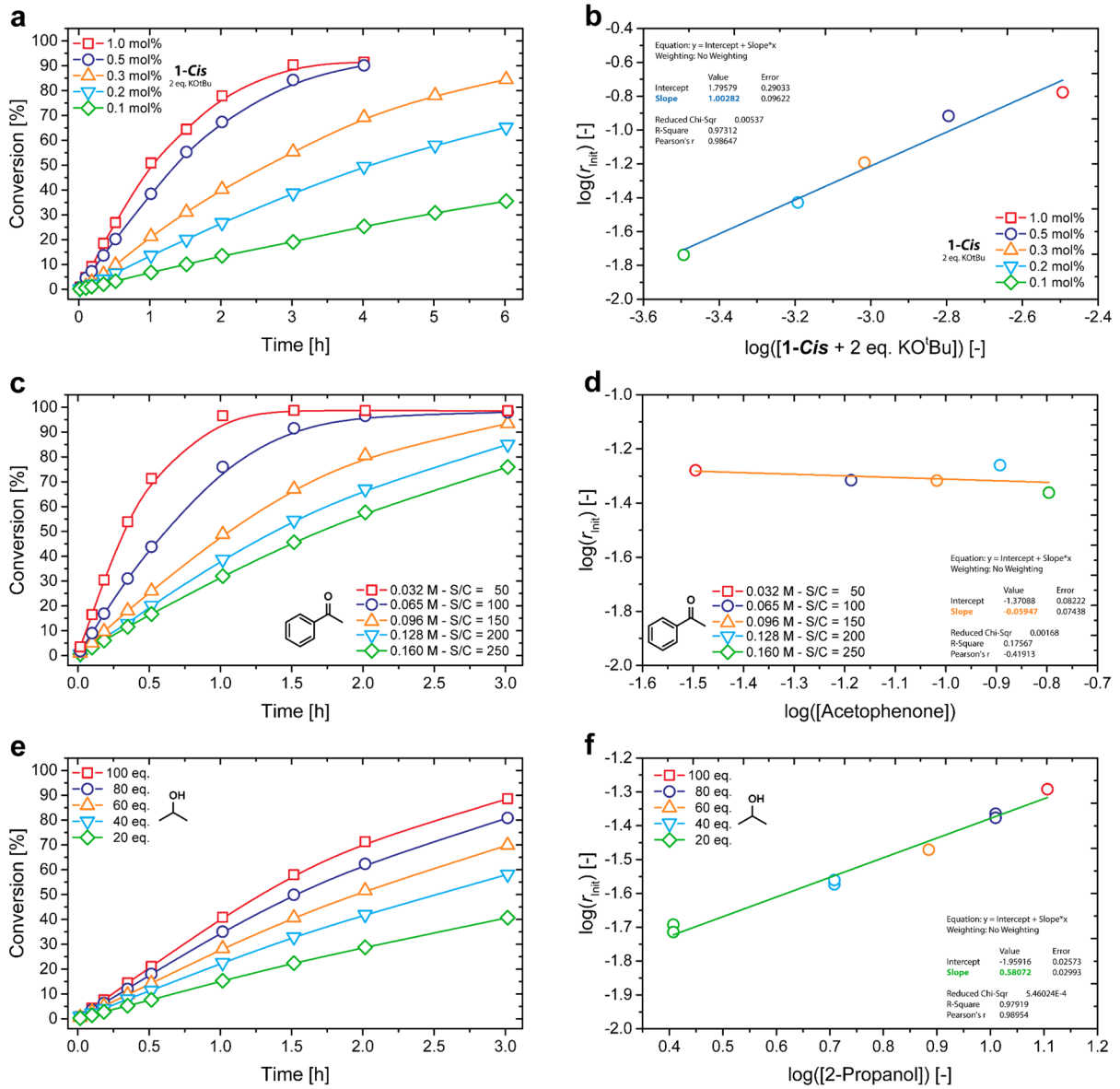

Figure 3. Kinetic reaction analysis of **1-*Cis*** catalyzed ATH of acetophenone. (a, b) Reaction order determination for **1-*Cis*** + 2 equiv of KO^{t}Bu. (c, d) Reaction order determination for acetophenone. (e, f) Reaction order determination for 2-propanol. Conditions unless otherwise noted: 0.5 mmol of acetophenone (0.128 M), 1.0 mol % KO^{t}Bu, 0.5 mol % **1-*Cis***, 3.82 mL of ^{i}PrOH (diluted with toluene for parts e and f), 60 °C. Yields determined by GC-FID using *n*-dodecane as an internal standard.

to be remarkably stable at temperatures tested up to 75 °C and does not produce any dehydrogenation products (e.g., acetone). This observation is in stark contrast to the behavior of aminopincer Mn−PNP or Mn−NHC complexes,[25,26] which are known to promote secondary alcohol dehydrogenation and typically form readily observable manganese−hydride complexes.[37] Complex **II**, however, reduces acetophenone to the corresponding alcohol, despite the notable absence of detectable hydride resonances in ^{1}H NMR (Figure S25). Furthermore, **II**−O^t**Bu** is resilient toward heterolytic hydrogen activation under basic conditions and did not form detectible amounts of Mn−hydride species upon pressurization with 3 bar of hydrogen gas.

We hypothesized that the introduction of more sterically demanding N-alkyl groups on the chiral ligand could improve the stereoselectivity. To test this hypothesis, complex **1-*Trans*−^{i}Pr** was prepared (Scheme 6). ATH of acetophenone with **1-*Trans*−^{i}Pr** led to the formation of (*R*)-1-phenylethanol with an identical ee of 71% as with **1-*Cis*** and **1-*Trans***, while catalytic activity was dramatically reduced to only one turnover (Table S2). Fully methylated complex **2** did not show any catalytic activity, therewith stressing the importance of accessible N*H* protons and confirming the proposed bifunctional mechanism involving protonation/deprotonation of the amino group of **1-*Cis*** and **1-*Trans***.

Compounds **1-*Cis*** and **1-*Trans*** are moderately enantioselective ketone transfer hydrogenation catalysts, which may be beneficial for future benchmarking of computational models and methods. We carried out a detailed kinetic analysis of the ATH using acetophenone as a model substrate with **1-*Cis***. At 60 °C, complex **1-*Cis*** (0.5 mol %) reacts with an initial turnover frequency of 79 h^{-1} and (*R*)-1-phenylethanol is produced quantitatively in 4 h with 73% ee. The initial reaction rates increase with increased catalyst loading (0.1−1.0 mol %

DOI: 10.1021/acs.organomet.9b00457
Organometallics 2019, 38, 3187−3196

Scheme 7. In-Situ Preparation and Detection of Mn−Alkoxide II−OPhEt

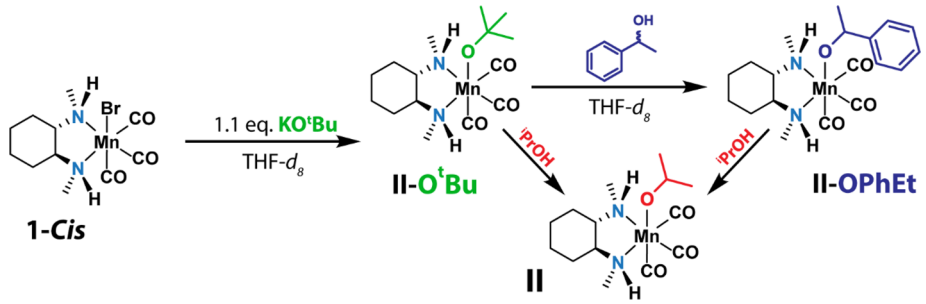

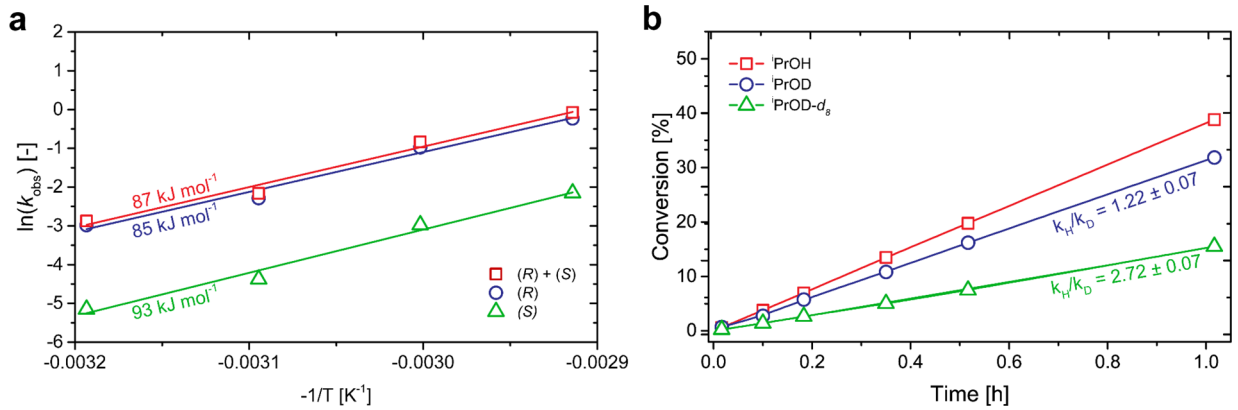

Figure 4. (a) Arrhenius plot for acetophenone ATH with **1-*Cis*** (left). (b) Kinetic isotope effect studies for ATH with **1-*Cis*** (right). Conditions: 0.5 mmol of acetophenone (0.128 M), 1.0 mol % KO^{t}Bu, 0.5 mol % **1-*Cis***, 3.82 mL of ^{i}PrOH or ^{i}PrOD, 40−70 °C. Yields determined by GC-FID using *n*-dodecane as an internal standard.

1-*Cis*) and are in agreement with a catalyst reaction order of 1.0 (Figure 3a,b and the Supporting Information). The influence of base concentration on precatalyst activation and the catalytic reaction rate was evaluated at various base loadings (see the Supporting Information). No effect is observed when 2−20 equiv of base relative to **1-*Cis*** was used, while lower base concentration resulted in reduced catalytic performance. Additionally, the catalyst reaction order in the presence of a large excess (5 mol %) of KO^{t}Bu similarly was equal to 1.0 (see the Supporting Information). Thus, all observations suggest that base solely acts as the precatalyst activator and does not play a significant role in the catalytic cycle for ATH.

The interpretation of kinetic data for acetophenone and ^{i}PrOH is less straightforward and revealed orders of 0 and 0.6, respectively (Figure 3c−f). Previously, Heeres and co-workers have derived a kinetic rate equation for the Ru-catalyzed ATH of ketones, taking into account effects caused by the reverse reaction (terms in the nominator), and effects due to catalyst inhibition by acetophenone (A), ^{i}PrOH (B), 1-phenylethanol (C), and acetone (D) (terms in the denominator), with parameters *k*, *m*, *n*, and *p*, as the reaction orders for inhibition caused by the respective reaction component (eq 1).[38]

$$-\frac{dC_A}{dt} = -r_A = \frac{k_1^+ C_A C_B - k_1^- C_C C_D}{1 + k_2 C_A^k + k_3 C_B^m + k_4 C_C^n + k_5 C_D^p} \quad (1)$$

$$-\frac{dC_A}{dt} = -r_A = \frac{k_1^+ C_A C_B}{1 + k_2 C_A^k + k_3 C_B^m} \quad (2)$$

At the start of the reaction, one can assume a negligible influence from the reverse reaction and its product (i.e., C and D), and the kinetic rate equation simplifies to eq 2. Both DFT and stoichiometric reactivity studies suggest a rapid reaction of the activated complex with ^{i}PrOH (B) to MnO^{i}Pr complex **II**. The *β*-H elimination step to convert **II** to Mn−hydride **III** and acetone is the rate-determining step (RDS) in the catalytic cycle. Subsequent elementary reactions lead to transfer of the hydride to acetophenone through a sequence of low-barrier transformations (Figure 2). This process is similar to conventional saturation kinetics[39] and is consistent with a zeroth order reaction rate in acetophenone, since the substrate is not involved in the RDS.

The predicted facile formation of Mn−alkoxide **II** also provides a rationalization for the positive fractional reaction order of the hydrogen donor and solvent, ^{i}PrOH. If inhibition by ^{i}PrOH is much faster than substrate inhibition (i.e., $k_3 C_B^m \gg 1 + k_2 C_A^k$) and C_A effectively is constant, eq 2 can be further reduced to eq 3. The extent of inhibition by ^{i}PrOH, as expressed in parameter *m*, directly impacts the observed reaction order in ^{i}PrOH, leading to the positive fractional reaction order value of 0.6 for ATH with **1-*Cis***.

$$-\frac{dC_A}{dt} = -r_A = \frac{k_1^+ C_A C_B}{k_3 C_B^m} = K_{obs} C_B^{1-m} \quad \text{with}$$

$$K_{obs} = \frac{k_1^+ C_A}{k_3} \quad (3)$$

The relative stability of Mn−alkoxide complexes in hydrogenations has been observed before by our group for closely related Mn−P,N complexes.[34,40] This led us to investigate the extent of product inhibition in ATH with **1-*Cis*** by means of additional stoichiometric reactivity studies. The Mn−1-

DOI: 10.1021/acs.organomet.9b00457
Organometallics 2019, 38, 3187−3196

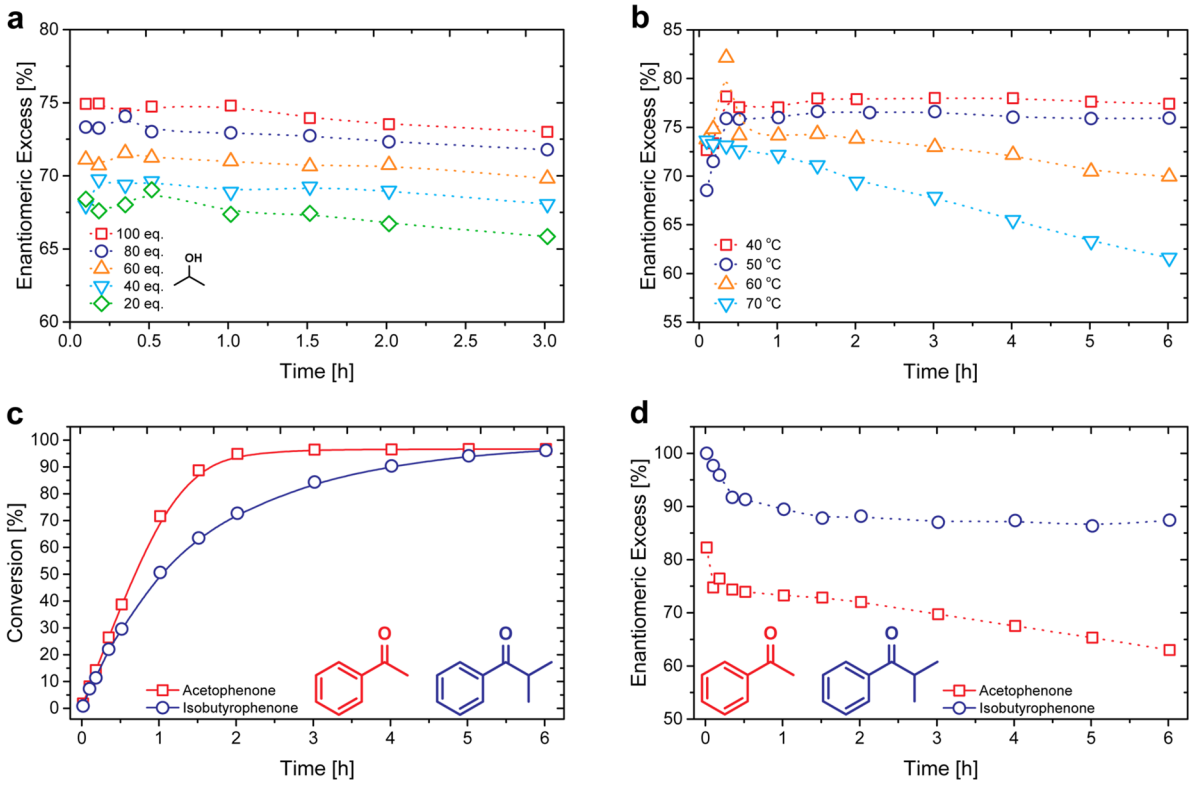

Figure 5. (a) Erosion of ee as a function of ^{i}PrOH concentration. (b) Erosion of ee as a function of reaction temperature. (c) Reaction rate of acetophenone and isobutyrophenone ATH with **1-*Cis***. (d) Erosion of ee for acetophenone and isobutyrophenone ATH. Conditions unless otherwise noted: 0.5 mmol of acetophenone (0.128 M), 1.0 mol % KO^{t}Bu, 0.5 mol % **1-*Cis*** (2.0 mol % KO^{t}Bu and 1.0 mol % **1-*Cis*** for parts c and d), 3.82 mL of ^{i}PrOH (diluted with toluene for parts a and b), 40−70 °C. Yields determined by GC-FID using *n*-dodecane as an internal standard.

phenylethoxide complex **II−OPhEt** was detected with ^{1}H NMR after reaction of **1-*Cis*** or **II−O^{t}Bu** with 1-phenylethanol and base (Scheme 7). Addition of ∼3 equiv of ^{i}PrOH led to the formation of a mixture of Mn−alkoxide complexes **II** and **II−OPhEt**, suggesting both may be present and that product inhibition cannot be ruled out in catalysis with **1-*Cis***.

In summary, catalyst inhibition by ^{i}PrOH is a significant process for the **1-*Cis***-catalyzed ATH of ketones and results in observed zeroth order kinetics for the substrate and a positive fractional reaction order for the hydrogen donor.

Activation Energies and KIE Measurements. We concluded our mechanistic studies with the determination of apparent activation energies and kinetic isotope effect (KIE) measurements to get a better experimental insight into the RDS. Acetophenone ATH with **1-*Cis*** proceeds with an apparent, nonasymmetric activation energy of 87 kJ mol^{-1} (Figure 4a). Detailed analysis of reaction rates allowed determination of the apparent E_A for the formation of individual (*R*) and (*S*) enantiomers, which is particularly useful for benchmarking computational models. The reaction to (*R*)-1-phenylethanol exhibits a barrier of 85 kJ mol^{-1}, while the pathway to (*S*)-1-phenylethanol proceeds with a marginally higher barrier of 93 kJ mol^{-1}. This observed $\Delta\Delta E_A^{App}$ of 8 kJ mol^{-1} for formation of both enantiomers corresponds well with the computed value of $\Delta\Delta G^{‡}$ for ATH of acetophenone with **1-*Cis*** (Scheme 4), with the overall observed and predicted barriers for the RDS showing some difference ($\Delta\Delta E$ of 15 kJ mol^{-1}; 70 kJ mol^{-1} from DFT versus experimental 85 kJ mol^{-1}). At this moment, however, it remains unclear what is the cause of this observed divergence between theory and experiments.

Studies in ^{i}PrOD-d_8 reveal a strong primary kinetic isotope effect (KIE) of 2.72 ± 0.07, consistent with hydride transfer from ^{i}PrOH being involved in the RDS of the catalytic cycle. This finding correlates well with the proposed mechanism (Figure 2), where *β*-hydride elimination from the coordinated isopropoxide ligand to form Mn−hydride **III** was identified as the most energetically demanding transformation. When ^{i}PrOD was used, we observed a secondary KIE of 1.22 ± 0.07 (Figure 4b). Proton transfer is clearly of less importance than hydride transfer, yet this process too has a clear impact on the rate-determining processes in the catalytic reaction mechanism.

ee Erosion and Preservation. The reversible nature of the transfer hydrogenation reaction of ketones with secondary alcohols as hydrogen donors is known to induce an erosion of product enantiomeric excess.[41] A strategy to prevent such ee erosion is to use an azeotropic mixture of formic acid and triethylamine as the hydrogen donor.[33,42] However, to the best of our knowledge, the reduction of ketones with 3d base metals and formic acid has not yet been reported. As with Ru-based systems,[41] we performed the reaction under dilute conditions in order to prevent the decrease of ee over time (Figure 5a). Indeed, in the presence of a large excess of ^{i}PrOH, erosion of ee was less pronounced. Increased reaction temperature resulted in significantly reduced product ee (Figure 5b).

We hypothesized that use of a more sterically demanding ketone substrate would lead to improved ee's compared to acetophenone (Figure 5c and d). Indeed, the ATH of isobutyrophenone under identical conditions results in quantitative production of (*R*)-2-methyl-1-phenylpropanol with 87% ee, albeit at a reduced reaction rate, i.e., ∼85%

DOI: 10.1021/acs.organomet.9b00457
Organometallics 2019, 38, 3187−3196

TOF^0 obtained with acetophenone reduction at 60 °C with 1 mol % **1-*Cis***.

CONCLUSION

In conclusion, we have synthesized and characterized a series of simple chiral manganese−diamine complexes which were evaluated for their catalytic performance in asymmetric transfer hydrogenation of acetophenones. Complexes **1-*Cis*** and **1-*Trans*** are stereoselective ATH catalysts for the synthesis of enantio-enriched secondary alcohols in good to quantitative yields. We conducted a detailed theoretical and experimental mechanistic investigation including the first detailed kinetic study for the Mn-catalyzed ATH of ketones. Our ligand screening revealed that introduction of simple diamine ligands does not induce sufficient steric strain to facilitate high enantioselectivity. We however found that such strain cannot practically be applied on the described Mn complexes bearing N-donors while concomitantly maintaining high catalytic activity. We demonstrated that different stereoisomeric precatalysts upon activation converge to shared intermediates and thus exhibit identical catalytic performance. This renders conventional approaches toward catalyst optimization unsuccessful and thus demands more thorough studies. Mechanistic insight and the recent applications of bidentate ligands containing a NHC group[14,25] suggest that introduction of a strongly donating but small bidentate ligand could lead to highly active and selective second-generation Mn catalysts for ATH of ketones.

ASSOCIATED CONTENT

Supporting Information

The Supporting Information is available free of charge on the ACS Publications website at DOI: 10.1021/acs.organomet.9b00457.

Experimental procedures and raw kinetic data (PDF)

Coordinates of optimized structures (XYZ)

Accession Codes

CCDC 1903883−1903885 contain the supplementary crystallographic data for this paper. These data can be obtained free of charge via www.ccdc.cam.ac.uk/data_request/cif, or by emailing data_request@ccdc.cam.ac.uk, or by contacting The Cambridge Crystallographic Data Centre, 12 Union Road, Cambridge CB2 1EZ, UK; fax: +44 1223 336033.

AUTHOR INFORMATION

Corresponding Author

*E-mail: E.A.Pidko@tudelft.nl.

ORCID

Robbert van Putten: 0000-0001-5074-6706

Georgy A. Filonenko: 0000-0001-8025-9968

Chong Liu: 0000-0003-0311-8744

Laurent Lefort: 0000-0003-2973-6540

Evgeny Pidko: 0000-0001-9242-9901

Present Address

$^{\perp}$C.L.: Institute for Catalysis, Hokkaido University, N-21, W-10, Sapporo, Japan.

Author Contributions

The manuscript was written through contributions of all authors. All authors have given approval to the final version of the manuscript.

Notes

The authors declare no competing financial interest.

ACKNOWLEDGMENTS

This project has been funded by the European Research Council (ERC) under the European Union's Horizon 2020 research and innovation programme (Grant Agreement No. 725686). We thank the students in our group Christophe Besnard and Joeri Benschop for their contributions to this work and the Ministry of Education and Science of the Russian Federation (Project 11.1706.2017/4.6) for partial support. The authors thank NWO Exact and Natural Sciences for providing access to the SurfSARA supercomputer facilities.

REFERENCES

(1) Bullock, R. M. Abundant Metals Give Precious Hydrogenation Performance. *Science* **2013**, *342* (6162), 1054−1055.

(2) Valyaev, D. A.; Lavigne, G.; Lugan, N. Manganese organometallic compounds in homogeneous catalysis: Past, present, and prospects. *Coord. Chem. Rev.* **2016**, *308* (2), 191−235.

(3) Filonenko, G. A.; van Putten, R.; Hensen, E. J. M.; Pidko, E. A. Catalytic (de)hydrogenation promoted by non-precious metals − Co, Fe and Mn: recent advances in an emerging field. *Chem. Soc. Rev.* **2018**, *47* (4), 1459−1483.

(4) Reed-Berendt, B. G.; Polidano, K.; Morrill, L. C. Recent advances in homogeneous borrowing hydrogen catalysis using earth-abundant first row transition metals. *Org. Biomol. Chem.* **2019**, *17*, 1595−1607.

(5) Garbe, M.; Junge, K.; Beller, M. Homogeneous Catalysis by Manganese-Based Pincer Complexes. *Eur. J. Org. Chem.* **2017**, *2017* (30), 4344−4362.

(6) Kallmeier, F.; Kempe, R. Manganese Complexes for (De)-Hydrogenation Catalysis: A Comparison to Cobalt and Iron Catalysts. *Angew. Chem., Int. Ed.* **2018**, *57* (1), 46−60.

(7) Gorgas, N.; Kirchner, K. Isoelectronic Manganese and Iron Hydrogenation/Dehydrogenation Catalysts: Similarities and Divergences. *Acc. Chem. Res.* **2018**, *51* (6), 1558−1569.

(8) Pritchard, J.; Filonenko, G. A.; van Putten, R.; Hensen, E. J. M.; Pidko, E. A. Heterogeneous and homogeneous catalysis for the hydrogenation of carboxylic acid derivatives: history, advances and future directions. *Chem. Soc. Rev.* **2015**, *44* (11), 3808−3833.

(9) Zuo, W.; Lough, A. J.; Li, Y. F.; Morris, R. H. Amine(imine)-diphosphine Iron Catalysts for Asymmetric Transfer Hydrogenation of Ketones and Imines. *Science* **2013**, *342* (6162), 1080−1083.

(10) Bielinski, E. A.; Förster, M.; Zhang, Y.; Bernskoetter, W. H.; Hazari, N.; Holthausen, M. C. Base-Free Methanol Dehydrogenation Using a Pincer-Supported Iron Compound and Lewis Acid Co-catalyst. *ACS Catal.* **2015**, *5* (4), 2404−2415.

(11) Bielinski, E. A.; Lagaditis, P. O.; Zhang, Y.; Mercado, B. Q.; Würtele, C.; Bernskoetter, W. H.; Hazari, N.; Schneider, S. Lewis Acid-Assisted Formic Acid Dehydrogenation Using a Pincer-Supported Iron Catalyst. *J. Am. Chem. Soc.* **2014**, *136* (29), 10234−10237.

(12) Fu, S.; Shao, Z.; Wang, Y.; Liu, Q. Manganese-Catalyzed Upgrading of Ethanol into 1-Butanol. *J. Am. Chem. Soc.* **2017**, *139* (34), 11941−11948.

(13) Maji, B.; Barman, M. K. Recent Developments of Manganese Complexes for Catalytic Hydrogenation and Dehydrogenation Reactions. *Synthesis* **2017**, *49* (15), 3377−3393.

(14) Buhaibeh, R.; Filippov, O. A.; Bruneau-Voisine, A.; Willot, J.; Duhayon, C.; Valyaev, D. A.; Lugan, N.; Canac, Y.; Sortais, J.-B. Phosphine-NHC Manganese Hydrogenation Catalyst Exhibiting a Non-Classical Metal-Ligand Cooperative H2 Activation Mode. *Angew. Chem., Int. Ed.* **2019**, *58* (20), 6727−6731.

(15) Misal Castro, L. C.; Li, H.; Sortais, J.-B.; Darcel, C. When iron met phosphines: a happy marriage for reduction catalysis. *Green Chem.* **2015**, *17* (4), 2283−2303.

DOI: 10.1021/acs.organomet.9b00457
Organometallics 2019, 38, 3187−3196

(16) Kallmeier, F.; Irrgang, T.; Dietel, T.; Kempe, R. Highly Active and Selective Manganese C = O Bond Hydrogenation Catalysts: The Importance of the Multidentate Ligand, the Ancillary Ligands, and the Oxidation State. *Angew. Chem., Int. Ed.* **2016**, *55* (39), 11806−11809.
(17) Dubey, A.; Nencini, L.; Fayzullin, R. R.; Nervi, C.; Khusnutdinova, J. R. Bio-Inspired Mn(I) Complexes for the Hydrogenation of CO2 to Formate and Formamide. *ACS Catal.* **2017**, *7* (6), 3864−3868.
(18) Perez, M.; Elangovan, S.; Spannenberg, A.; Junge, K.; Beller, M. Molecularly Defined Manganese Pincer Complexes for Selective Transfer Hydrogenation of Ketones. *ChemSusChem* **2017**, *10* (1), 83−86.
(19) Bruneau-Voisine, A.; Wang, D.; Dorcet, V.; Roisnel, T.; Darcel, C.; Sortais, J.-B. Transfer Hydrogenation of Carbonyl Derivatives Catalyzed by an Inexpensive Phosphine-Free Manganese Precatalyst. *Org. Lett.* **2017**, *19* (13), 3656−3659.
(20) Martínez-Ferraté, O.; Werlé, C.; Franciò, G.; Leitner, W. Aminotriazole Mn(I) Complexes as Effective Catalysts for Transfer Hydrogenation of Ketones. *ChemCatChem* **2018**, *10* (20), 4514−4518.
(21) Shvydkiy, N. V.; Vyhivskyi, O.; Nelyubina, Y.; Perekalin, D. Design of manganese phenol pi-complexes as Shvo-type catalysts for transfer hydrogenation of ketones. *ChemCatChem* **2019**, *11* (6), 1602−1605.
(22) Ganguli, K.; Shee, S.; Panja, D.; Kundu, S. Cooperative Mn(I)-complex catalyzed transfer hydrogenation of ketones and imines. *Dalton Trans* **2019**, *48*, 7358−7366.
(23) Dubey, A.; Rahaman, S. M. W.; Fayzullin, R. R.; Khusnutdinova, J. Transfer hydrogenation of carbonyl groups, imines and N-heterocycles catalyzed by simple, bipyridine-based MnI complexes. *ChemCatChem* **2019**, DOI: 10.1002/cctc.201900358.
(24) Wei, D.; Bruneau-Voisine, A.; Dubois, M.; Bastin, S.; Sortais, J.-B. Manganese-Catalyzed Transfer Hydrogenation of Aldimines. *ChemCatChem* **2019**, DOI: 10.1002/cctc.201900314.
(25) van Putten, R.; Benschop, J.; de Munck, V.; Weber, M.; Mueller, C.; Filonenko, G.; Pidko, E. A. Efficient and practical transfer hydrogenation of ketones catalyzed by a simple bidentate Mn-NHC complex. *ChemCatChem* **2019**, DOI: 10.1002/cctc.201900882.
(26) Zirakzadeh, A.; de Aguiar, S. R. M. M.; Stöger, B.; Widhalm, M.; Kirchner, K. Enantioselective Transfer Hydrogenation of Ketones Catalyzed by a Manganese Complex Containing an Unsymmetrical Chiral PNP′ Tridentate Ligand. *ChemCatChem* **2017**, *9*, 1744−1748.
(27) Widegren, M. B.; Harkness, G. J.; Slawin, A. M. Z.; Cordes, D. B.; Clarke, M. L. A Highly Active Manganese Catalyst for Enantioselective Ketone and Ester Hydrogenation. *Angew. Chem., Int. Ed.* **2017**, *56*, 5825−5828.
(28) Garbe, M.; Junge, K.; Walker, S.; Wei, Z.; Jiao, H.; Spannenberg, A.; Bachmann, S.; Scalone, M.; Beller, M. Manganese-(I)-Catalyzed Enantioselective Hydrogenation of Ketones Using a Defined Chiral PNP Pincer Ligand. *Angew. Chem., Int. Ed.* **2017**, *56* (37), 11237−11241.
(29) Schneekönig, J.; Junge, K.; Beller, M. Manganese Catalyzed Asymmetric Transfer Hydrogenation of Ketones Using Chiral Oxamide Ligands. *Synlett* **2019**, *30* (04), 503−507.
(30) Demmans, K. Z.; Olson, M. E.; Morris, R. H. Asymmetric Transfer Hydrogenation of Ketones with Well-Defined Manganese(I) PNN and PNNP Complexes. *Organometallics* **2018**, *37* (24), 4608−4618.
(31) Wang, D.; Bruneau-Voisine, A.; Sortais, J.-B. Practical (asymmetric) transfer hydrogenation of ketones catalyzed by manganese with (chiral) diamines ligands. *Catal. Commun.* **2018**, *105*, 31−36.
(32) Magano, J.; Dunetz, J. R. Large-Scale Carbonyl Reductions in the Pharmaceutical Industry. *Org. Process Res. Dev.* **2012**, *16* (6), 1156−1184.
(33) Wang, D.; Astruc, D. The Golden Age of Transfer Hydrogenation. *Chem. Rev.* **2015**, *115* (13), 6621−6686.
(34) van Putten, R.; Uslamin, E. A.; Garbe, M.; Liu, C.; Gonzalez-De-Castro, A.; Lutz, M.; Junge, K.; Hensen, E. J. M.; Beller, M.; Lefort, L.; Pidko, E. A. Non-Pincer-Type Manganese Complexes as Efficient Catalysts for the Hydrogenation of Esters. *Angew. Chem., Int. Ed.* **2017**, *56* (26), 7531−7534.
(35) Langer, R.; Diskin-Posner, Y.; Leitus, G.; Shimon, L. J. W.; Ben-David, Y.; Milstein, D. Low-Pressure Hydrogenation of Carbon Dioxide Catalyzed by an Iron Pincer Complex Exhibiting Noble Metal Activity. *Angew. Chem., Int. Ed.* **2011**, *50* (42), 9948−9952.
(36) Frisch, M.; Trucks, G.; Schlegel, H.; Scuseria, G.; Robb, M.; Cheeseman, J.; Scalmani, G.; Barone, V.; Mennucci, B.; Petersson, G. *Gaussian 09*, revision D.01; Gaussian, Inc.: Wallingford, CT, 2009.
(37) Nguyen, D. H.; Trivelli, X.; Capet, F.; Paul, J.-F.; Dumeignil, F.; Gauvin, R. M. Manganese Pincer Complexes for the Base-Free, Acceptorless Dehydrogenative Coupling of Alcohols to Esters: Development, Scope, and Understanding. *ACS Catal.* **2017**, *7* (3), 2022−2032.
(38) Wisman, R. V.; de Vries, J. G.; Deelman, B.-J.; Heeres, H. J. Kinetic Studies on the Asymmetric Transfer Hydrogenation of Acetophenone Using a Homogeneous Ruthenium Catalyst with a Chiral Amino-Alcohol Ligand. *Org. Process Res. Dev.* **2006**, *10* (3), 423−429.
(39) Swiegers, G. F. *Mechanical Catalysis: Methods of Enzymatic, Homogeneous, and Heterogeneous Catalysis*; John Wiley & Sons, Inc.: 2008.
(40) Liu, C.; van Putten, R.; Kulyaev, P. O.; Filonenko, G. A.; Pidko, E. A. Computational insights into the catalytic role of the base promoters in ester hydrogenation with homogeneous non-pincer-based Mn-P,N catalyst. *J. Catal.* **2018**, *363*, 136−143.
(41) Hashiguchi, S.; Fujii, A.; Takehara, J.; Ikariya, T.; Noyori, R. Asymmetric Transfer Hydrogenation of Aromatic Ketones Catalyzed by Chiral Ruthenium(II) Complexes. *J. Am. Chem. Soc.* **1995**, *117* (28), 7562−7563.
(42) Fujii, A.; Hashiguchi, S.; Uematsu, N.; Ikariya, T.; Noyori, R. Ruthenium(II)-Catalyzed Asymmetric Transfer Hydrogenation of Ketones Using a Formic Acid-Triethylamine Mixture. *J. Am. Chem. Soc.* **1996**, *118* (10), 2521−2522.

DOI: 10.1021/acs.organomet.9b00457
Organometallics 2019, 38, 3187−3196